Al-Qadisiyah Journal For Engineering Sciences 19 (2026) 195 – 202

Contents lists available at: http://qu.edu.iq

Al-Qadisiyah Journal for Engineering Sciences

Journal homepage: https://qjes.qu.edu.iq

Research Paper

Effect of ground granulated blast furnace slag–stabilized bentonite soils on flexible pavement design and cost analysis

Bahadır Karabaş [1] ***and Ali Ulvi Uzer*** [2]

[1] *İnönü University, Department of Civil Engineering, İnönü University, Malatya, Turkey.*
[2] *Kayseri University, Department of Construction, Vocational School of Technical Sciences, Kayseri University, Kayseri, Turkey.*

ARTICLE INFO

Article history:
Received 06 February 2026
Received in revised form 21 April 2026
Accepted 12 June 2026

keywords:
Ground granulated blast furnace slag
Bentonite clay
Soil stabilization
Flexible pavement design
Transportation geotechnics
AASHTO 1993

ABSTRACT

In this study, the effects of ground granulated blast furnace slag (GGBFS) stabilization of subgrade soil on flexible pavement layer thicknesses and initial construction costs were investigated. For this purpose, Proctor compaction tests were conducted on bentonite (BT) soil samples prepared by adding GGBFS at rates of 5%, 10%, 15%, and 20% by weight. Following these tests, unconfined compressive strength specimens were prepared and tested after curing periods of 3 and 7 days. The results indicated that the highest compressive strength was obtained in mixtures containing 15% GGBFS. In addition, untreated soil and soil samples stabilized with 15% GGBFS were subjected to the California Bearing Ratio (CBR) test after 3 and 7 days of curing. It was determined that the CBR values of the samples containing 15% GGBFS increased by 2.09 and 2.85 times, respectively. Using the CBR values obtained, pavement layer thicknesses were calculated based on the AASHTO 1993 flexible pavement design guidelines, and cost analyses were performed. The results showed that stabilization with 15% GGBFS reduced the initial construction costs by 23.03%.

1. Introduction

Throughout the historical development of societies, the needs for shelter and transportation have always been among the primary engineering challenges. In particular, highways, which are one of the most important components of transportation infrastructure, must be constructed under diverse climatic conditions and in various geographical regions. However, previous studies have shown that subgrade soils do not always possess the desired engineering properties. Problems such as low bearing capacity, high plasticity, and excessive compressibility can directly and adversely affect pavement performance. Therefore, economical and safe highway design can only be achieved through the proper improvement of subgrade soils using appropriate methods. Soil stabilization refers to a set of techniques applied to enhance the engineering properties of soils with low bearing capacity. Traditionally, materials such as lime, cement, and bitumen have been used in stabilization practices [1–4]. However, in recent years, due to concerns regarding environmental sustainability and economic efficiency, the use of industrial by-products and waste materials in soil improvement has increased significantly [5–14, 14]. Rahgozar et al. [11] determined that the addition of 4% cement and 10% rice husk ash represented the optimum mixture ratio based on the results of unconfined compressive strength tests conducted to improve clay soils. Zorluer and Gucek [11] investigated the usability of industrial wastes in soil improvement and reported that these materials are advantageous in terms of both economic and environmental aspects. Geçkil et al. [12, 13] examined the stabilization of clayey sand soils using carbon black obtained from waste vehicle tires. They reported increases in California Bearing Ratio (CBR) values by 1.28, 1.77, and 2.87 times after curing periods of 1, 7, and 28 days, respectively, with the addition of 10% carbon black. Perera et al. [14] conducted a series of mechanical and microstructural analyses by adding crushed glass to clay soils at different proportions (0%, 5%, 10%, 15%, and 20%). According to the experimental results, the addition of crushed glass at rates of 10–15% significantly improved mechanical properties such as unconfined compressive strength, CBR, and elastic modulus, reduced swelling and shrinkage potentials, and increased the water retention capacity of the clay. Domphoeun and Eisazadeh [15] stabilized soils using rice husk ash, coconut fiber, and lime. Modified Proctor, unconfined compressive strength, liquid limit, and plastic limit tests were performed on samples prepared with 0%, 5%, 10%, 15%, and 20% rice husk ash, coconut fiber, and lime contents. According to the test results, the mixture containing 20% rice husk ash, 1% coconut fiber, and 8% lime provided the optimum stabilization performance. Among industrial waste materials, blast furnace slag is a by-product of the iron and steel industry that contains high amounts of silica, alumina, and calcium oxide. It exhibits pozzolanic properties by reacting with soil and has been reported to be suitable for the stabilization of various soil types [16–21]. Sivrikaya et al. [16] emphasized this suitability by demonstrating that the addition of ground granulated blast furnace slag (GGBFS) reduced the plasticity index and improved the compaction parameters of clay soils. Abdila et al. [17] reported that GGBFS increased the CBR values of stabilized soils and also evaluated their compaction characteristics by determining the optimum moisture content and maximum dry unit weight through Proctor compaction tests. Soğancı et al. [18] stated that the use of GGBFS-stabilized soils in flexible pavement design resulted in lower maintenance costs and minimized long-term environmental impacts . Tomaz et al. [19] found that GGBFS improved compaction parameters and contributed to the formation of a more stable subgrade. In addition, triaxial compression tests were identified as an important method for determining the shear strength parameters of soils after stabilization. These tests revealed that GGBFS enhanced long-term strength by increasing cohesion and internal friction angle. Hu et al. [20] demonstrated that combinations of blast furnace slag and fly ash, optimized using machine learning approaches, provided optimum strength and deformation characteristics in flexible pavement design.

*Corresponding Author.
E-mail address: karabasbaha@gmail.com ; Tel: (+90) 542-425 8350 (Bahadır Karabaş)

https://doi.org/10.30772/qjes.2026.169263.1896
2411-7773

Nomenclature

M_R	Effective modulus of subgrade reaction for the subgrade soil (psi)	P_o	initial serviceability index
P_t	terminal serviceability index	*Greek Symbols*	
q	axial stress	ω_{opt}	Optimum moisture content
q_u	unconfined compressive strength	ω_L	Liquid limit
S_o	composite standard error of the performans traffic prediction	ΔPSI	Total serviceability loss
SN	structural number (used for pavement layer thickness calculation)	ρ_{dmax}	Maximum dry density
$T_{8.2}$	number of repetitions of the single axle load (ESAL) of 8.2 tons for the design traffic	ρ_s	Particle density
Z_R	standard normal deviate	ε	Axial strain at failure

Uzer et al. [21] reported that blast furnace slag- and fly ash-based geopolymers ensured sustainable stabilization of clay soils and that the results modeled using artificial neural networks confirmed the observed strength improvements. In conclusion, ground granulated blast furnace slag (GGBFS) emerges as a promising alternative for the improvement of subgrade soils in flexible pavement design. Although studies on GGBFS have generally focused on mechanical improvement, it has been observed that the direct effects of using GGBFS in the stabilization of bentonite-type clays with high plasticity on pavement layer thicknesses and initial construction costs have not been sufficiently detailed in the literature. In particular, integrating technical improvements with economic data during the design stage is considered to be of critical importance for engineering decision-making. In this study, unlike previous research that has mainly focused on the strength parameters of stabilized soils, a holistic approach is presented by integrating geotechnical improvement with pavement design optimization and economic feasibility. By focusing on bentonite clay, which is a highly challenging subgrade material from an engineering perspective, this study reveals the reduction in pavement layer thicknesses achieved through GGBFS stabilization in accordance with the AASHTO 1993 guidelines. For this purpose, soil samples considered as subgrade were stabilized by adding GGBFS at rates of 5%, 10%, 15%, and 20% by weight. Standard Proctor compaction, unconfined compressive strength, and California Bearing Ratio (CBR) tests were conducted on both untreated and stabilized samples. Flexible pavement design was performed based on the AASHTO 1993 guidelines, and the resulting pavement layer thicknesses and cost analyses were evaluated. Within this scope, the cost analysis indicates that this study fills an important gap in the literature regarding the practical and economic feasibility of GGBFS-stabilized bentonite subgrades in sustainable highway infrastructure.

Table 1. Properties of bentonite.

Soil Property	Symbol	Value	Unit	ASTM
Optimum Moisture Content	ω_{opt}	35.25	%	D698
Maximum Dry Density	ρ_{dmax}	1.310	g/cm^3	D698
Bulk Density	ρ_s	0.9	g/cm^3	D854
Liquid Limit	ω_L	350-450	%	D4318
Sieve Residue on 150 μm Sieve	—	2.50	%	D6913
Sieve Residue on 75 μm Sieve	—	12.5	%	D6913
Unified Soil Classification System	USCS	CH	—	D6913

Table 2. Chemical composition of bentonite .

Component	Value (%)
Na_2O	2.41
MgO	2.68
Al_2O_3	16.54
SiO_2	63.40
P_2O_5	0.13
SO_3	0.41
Cl	0.03
K_2O	1.10
$CaCO_3$	6.91
TIO_2	0.76
V_2O_5	0.02
Cr_2O_3	0.02
MnO	0.08
Fe_2O_3	5.51

2. Materials and methods

2.1 Subgrade soil (sodium bentonite)

In this study, the subgrade soil was evaluated as sodium bentonite (BT), a clay mineral known for its high plasticity, significant swelling potential, low shear strength, and high compressibility. These characteristics can cause serious engineering problems, such as foundation settlement, loss of bearing capacity, and damage related to swelling–shrinkage behavior. The main component of bentonite is montmorillonite, and according to the Unified Soil Classification System (USCS), it is classified as high-plasticity clay (CH). The sodium bentonite samples used in this study were obtained from Çanbensan Çankırı Bentonit San. Tic. A.S. In accordance with the relevant standards [22–25], the properties of the prepared samples are presented in Table 1, their chemical composition is given in Table 2, and their physical appearance is shown in Fig. 1.

Figure 1. Physical appearance of the bentonite sample.

2.2 Ground granulated blast furnace slag

Ground granulated blast furnace slag (GGBFS) is an industrial by-product obtained by rapidly quenching molten slag from blast furnaces in the iron and steel industry with water to form granules, which are then finely ground. It possesses hydraulic binding properties. Due to its high content of calcium oxide (CaO), silicon dioxide (SiO_2), and aluminum oxide (Al_2O_3), GGBFS undergoes pozzolanic reactions, exhibiting cementitious behavior. These properties make GGBFS widely used as a cement replacement, in geopolymer production, and as an eco-friendly alternative binder in soil stabilization. Previous studies have demonstrated that GGBFS improves both engineering performance and reduces carbon emissions [18–21]. The GGBFS used in the experiments is a by-product of İskenderun Iron and Steel Factory. Its chemical composition is presented in Table 3, and a sample is shown in Fig. 2.

Figure 2. Physical appearance of the GGBFS sample.

Table 3. Chemical composition of GGBFS.

Component	Value (%)
CaO	33.6
SiO_2	41.2
Al_2O_3	14.3
MgO	7.3
S	0.8
MnO	0.8
K_2O	0.9
TIO_2	1.1

2.3 Standard proctor, unconfined compressive strength, and California bearing ratio tests

The Standard Proctor test is one of the fundamental laboratory methods used to determine the compaction characteristics of soils. This test provides the maximum dry density (ρ_{dmax}) and optimum moisture content (ω_{opt}) of the soil and is conducted in accordance with ASTM D698 [23]. The cylindrical mold used in the test has a diameter of approximately 105 mm and a height of 115.5 mm. Soil samples are oven-dried at 105°C for 24 hours and then prepared with varying moisture contents. The prepared samples are placed in the mold in three layers, and each layer is compacted with 25 blows using a 2.5 kg hammer. After placing the final layer, the surface is leveled, and the sample weight is recorded. This procedure is repeated five times for different moisture contents. For each trial, the dry density is calculated and correlated with the corresponding moisture content. The obtained data are used to plot the compaction curve, from which the maximum dry density and optimum moisture content of the soil are determined [26]. The unconfined compressive strength (UCS) test is conducted to determine the strength of soil samples prepared according to ASTM D2166 [27] after specific curing periods. During the test, soil samples are oven-dried at 105°C for 24 hours. The dimensions of the cylindrical mold (38 *mm* in diameter and 76 *mm* in height) are measured and checked prior to testing. Samples are prepared by adding predetermined amounts of water and placed into the mold in four layers. Each layer is compacted by applying 10 blows with a tamping rod. After compaction, the sample is carefully removed from the mold and allowed to cure at room temperature for the specified period. During the test, the axial strain rate should be maintained between 0.5% and 2% per minute. At the end of the test, the ultimate strength and corresponding deformations are recorded to determine the unconfined compressive strength of the samples [28]. In this study, UCS tests were performed on both soil and mixture samples following ASTM D2166, after 3 and 7 days of curing. The California Bearing Ratio (CBR) test, conducted in accordance with ASTM D1883-13, is used to determine the bearing capacity of soil samples prepared based on the previously determined maximum dry density and optimum moisture content, after the specified curing period. During the test, a piston with an area of 1935 mm^2 is penetrated into the soil at a rate of 1.27 mm/min. The CBR value is calculated as the ratio of the applied load on the soil at specific penetration depths (2.5 *mm* and 5 *mm*) to the load applied to a standard crushed rock sample at the same penetration depths. The dimensions of the mold used in the test are measured and recorded. The prepared sample is placed into the CBR mold in three layers, and each layer is compacted with 56 blows using a tamping rod. After compaction, the mold containing the sample is weighed to verify density values. Following the specified curing period, the samples are placed in the testing apparatus. CBR values are then calculated for 2.5 *mm* and 5 *mm* penetration depths [29]. The application stages of the CBR test are illustrated in Fig. 3.

2.4 Flexible pavement design

Flexible pavement design consists of asphalt concrete surfacing, base, and subbase layers. During the construction of these layers, asphalt binder is used as the primary binding material. In the design process, various factors are considered, including service life, layer thicknesses, traffic intensity, regional conditions, economic factors, and subgrade soil properties [30,31]. Figure 4 illustrates the layers of the flexible pavement. The layer thicknesses are calculated according to the AASHTO 1993 guidelines using Eq. 1.

$$\log(T_{8.2}) = Z_R \times S_o + 9.36 \times \log(SN+1) + \frac{\log\frac{\Delta PSI}{2.7}}{0.4 + \frac{1094}{(SN+1)^{5.19}}} + 2.32 \times \log M_R - 8.27 \quad (1)$$

After the *SN* value is determined using Eq. 1, the pavement layer thicknesses are calculated using Eq. 2 based on the layer coefficients [31].

$$SN = a_1 \times D_1 + a_2 \times D_2 \times M_2 + a_3 \times D_3 \times M_3 \ldots\ldots\ldots\ldots a_i \times D_i \quad (2)$$

Here, a_1, a_2, and a_3 represent the relative strength coefficients of the surface course, base course, and subbase course, respectively, while D_1, D_2, and D_3 denote the thicknesses of the surface, base, and subbase layers. M_2 and M_3 indicate the drainage coefficients of the base and subbase layers. After the calculation of the layer thicknesses, the layer thicknesses are verified and adjusted using the SN^* values according to the procedure shown in Figure 5. In Figure 5, the SN_3, SN_2, and SN_1 represent the required structural numbers for the subgrade, subbase, and base courses, respectively, and the asterisk (∗) indicates the values corresponding to the materials used [31].

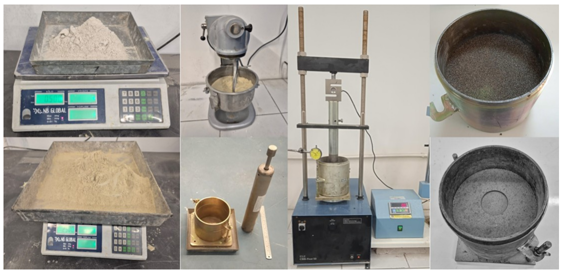

Figure 3. Application stages of the CBR test.

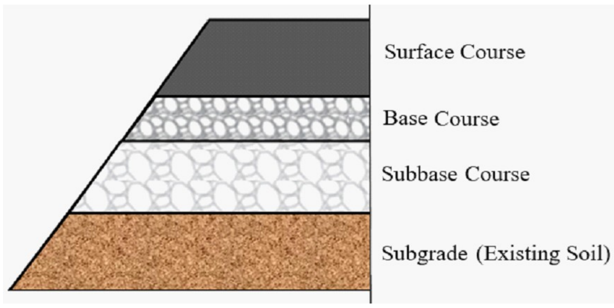

Figure 4. Cross-section of the flexible pavement [32].

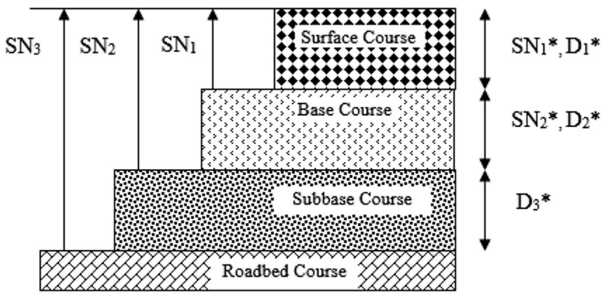

Figure 5. Structural numbers (SN) in flexible pavement design [31].

3. Research findings and discussion

In this study, the effects of stabilizing the subgrade soil with GGBFS on flexible pavement performance were investigated. The results of laboratory tests and pavement design outputs are presented as follows:

3.1 Standard proctor test results

Standard Proctor tests were performed on bentonite (BT) samples and mixtures containing 5%, 10%, 15%, and 20% GGBFS by weight. The tests were conducted on specimens prepared at five different moisture contents for both bentonite soil and GGBFS-containing mixtures. Based on the measured dry density and moisture content results, the compaction curves are illustrated in Fig. 6. The determined maximum dry density and optimum moisture content values are presented in Table 4. Upon examining the Standard Proctor test results, it was observed that increasing the GGBFS content led to an increase in ω_{opt} and a decrease in ρ_{dmax}, and the results were consistent with those reported in the literature [33–36]. This behavior is in agreement with previous studies [35,37], which suggest that the low specific gravity of GGBFS, its porous granular structure, and the increase in interparticle voids reduce the compactibility of the mixture, thereby requiring more water to achieve optimum compaction.

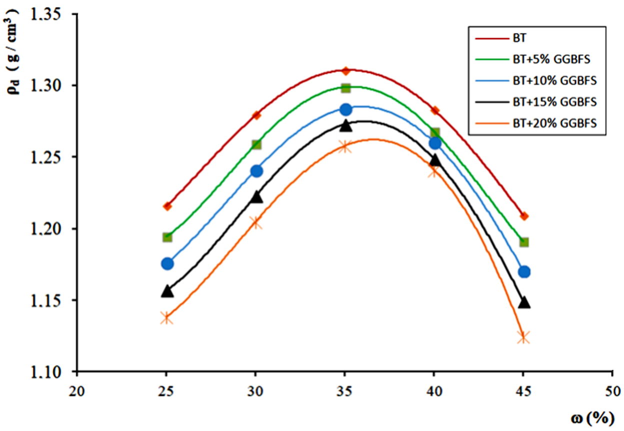

Figure 6. Compaction curves from the standard proctor test.

Table 4. Standard proctor test results for BT and GGBFS mixtures.

Test Samples	ρ_{dmax} (g/cm^3)	$\omega_{opt}(\%)$
BT	1.310	35.25
BT+5% GGBFS	1.297	35.63
BT+10% GGBFS	1.285	36.05
BT+15% GGBFS	1.274	36.44
BT+20% GGBFS	1.261	36.85

3.2 Unconfined compressive strength test results

Unconfined compressive strength (UCS) test samples, consisting of bentonite (BT) mixed with 5%, 10%, 15%, and 20% GGBFS by weight, were prepared based on the previously determined maximum dry density and optimum moisture content. For each mixture, three specimens were prepared and stored at room temperature. The samples were subjected to UCS tests after curing periods of 3 and 7 days, and the average values were reported. The axial stress (q) versus axial strain (ε) results for the untreated soil and GGBFS-stabilized samples are presented in Fig. 7 and Fig. 8. In addition, the unconfined compressive strength (q_u) and the axial strain at failure (ε) are given in Table 5 and Table 6.

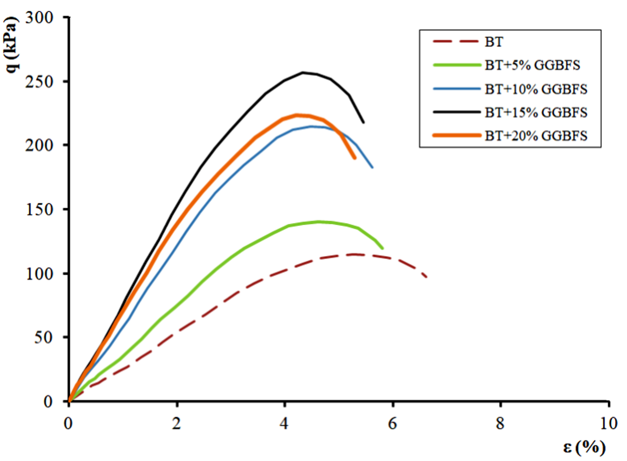

Figure 7. Axial stress–strain (q–ε) curves of BT and GGBFS mixtures after 3 days of curing.

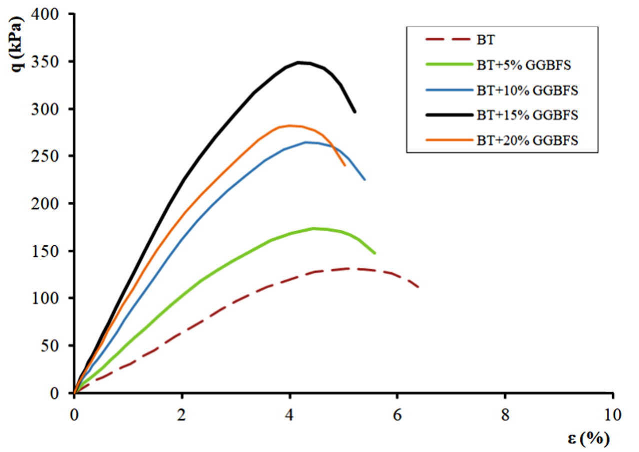

Figure 8. Axial stress–strain (q–ε) curves of BT and GGBFS mixtures after 7 days of curing.

Table 5. Unconfined compressive strength and axial strain of BT–GGBFS mixtures after 3 days curing.

Test Samples	q_u (Kpa)	$\varepsilon_u(\%)$
BT	114.69	5.26
BT+5% GGBFS	140.23	4.61
BT+10% GGBFS	214.77	4.47
BT+15% GGBFS	256.43	4.33
BT+20% GGBFS	223.65	4.21

Table 6. Unconfined compressive strength and axial strain of BT–GGBFS mixtures after 7 days curing.

Test Samples	q_u (Kpa)	$\varepsilon_u(\%)$
BT	131.35	5.07
BT+5% GGBFS	173.56	4.43
BT+10% GGBFS	264.88	4.28
BT+15% GGBFS	348.88	4.14
BT+20% GGBFS	282.29	3.99

Upon examining the unconfined compressive strength (UCS) test results, it was observed that the UCS values of the unamended BT samples were lower than those of the GGBFS-stabilized mixtures after 3 and 7 days of curing, indicating that GGBFS improved the strength of the mixtures. The highest strength was observed in the samples containing 15% GGBFS. At this content, the UCS values increased by factors of 2.24 and 2.66 compared to the unamended BT samples after 3 and 7 days of curing, respectively. The increase in strength due to GGBFS addition is consistent with the literature [33–36]. Moreover, increasing the GGBFS content and curing period led to a reduction in axial strain, which is associated with an increase in the stiffness of the samples. This observation is also in agreement with the findings reported in the literature [38].

3.3 California bearing ratio test results

For the CBR tests, specimens were prepared using untreated BT, and the mixture containing the optimum 15% GGBFS was identified based on the UCS test results. The samples were molded in accordance with the maximum dry density and optimum moisture content values. During the 3 and 7-day curing periods, the specimens were kept at room temperature under controlled conditions and protected from external effects. Following the curing process, dry CBR tests were performed. The load–penetration relationships obtained from these tests are illustrated in Fig. 9 and Fig. 10, and the corresponding CBR values are summarized in Table 7 and Table 8. Upon examining the CBR test results, it was observed that the addition of GGBFS increased the CBR values of the mixtures. For the 15% GGBFS mixtures, the CBR values at 2.5 mm and 5 mm penetration were 9.78% and 10.80%, respectively, after 3 days of curing, and 13.97% and 15.43%, respectively, after 7 days of curing. Compared to the unamended BT samples, the CBR values of the GGBFS-stabilized mixtures were increased by factors of 2.06 and 2.09 after 3 days, and 2.64 and 2.85

after 7 days, for 2.5 mm and 5 mm penetration, respectively. The higher CBR values of the GGBFS-stabilized mixtures compared to the unamended soil are consistent with the literature [21, 33, 34, 36], which indicates that GGBFS improves the bearing capacity of soils. Previous studies report that the reactive components of GGBFS, including calcium, silica, and alumina, promote the formation of binder hydration products between soil particles, leading to densification of the soil microstructure, increased mechanical strength, and controlled volumetric behavior. Due to its hydraulic and pozzolanic properties, GGBFS acts as an effective binder, playing a key role in stabilizing highly plastic clays that otherwise exhibit low strength and pose significant engineering problems. In this study, the applied GGBFS was found to enhance the strength of the mixtures and improve their mechanical properties. However, it was also observed that adding GGBFS beyond the determined optimum content did not further increase the strength, likely because the excess GGBFS remained unreacted.

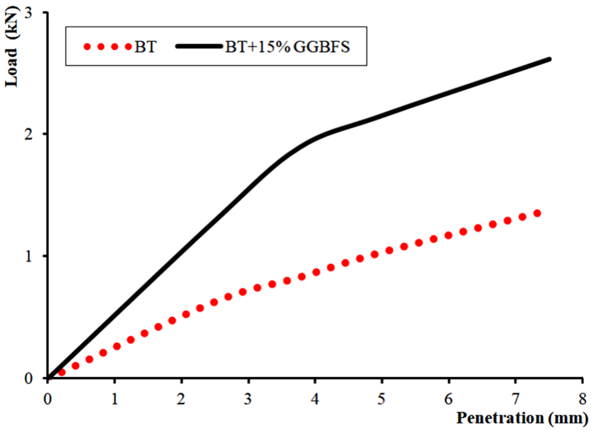

Figure 9. Load–penetration curves of unamended BT and 15% GGBFS mixtures after 3 days of curing.

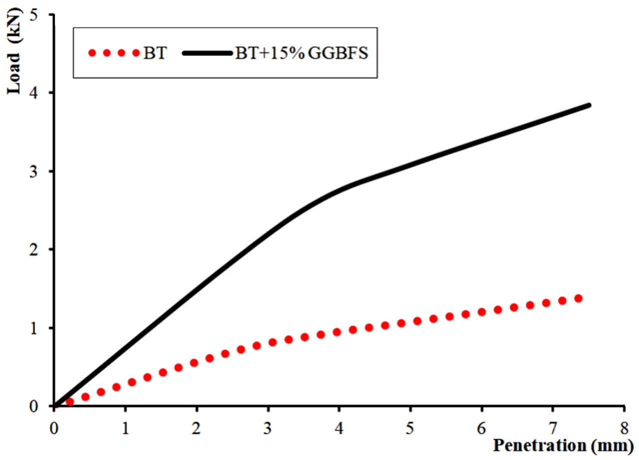

Figure 10. Load–penetration curves of unamended BT and 15% GGBFS mixtures after 7 days of curing.

Table 7. CBR values of unamended BT and 15% GGBFS mixtures after 3 days of curing.

Test Samples	CBR Value at 2.5 mm Penetration (%)	CBR Value at 5 mm Penetration (%)
BT	4.74	5.17
%15 GGBFS	9.78	10.80

Table 8. CBR values of unamended BT and 15% GGBFS mixtures after 7 days of curing.

Test Samples	CBR Value at 2.5 mm Penetration (%)	CBR Value at 5 mm Penetration (%)
BT	5.29	5.41
%15 GGBFS	13.97	15.43

3.4 Flexible pavement design

The flexible pavement design was carried out according to the principles outlined in AASHTO 1993, based on the CBR values determined after 3 and 7 days of curing. For the design, the highest CBR value obtained at the 7-day curing period was used. The reference CBR values were 5.41% for the unamended BT and 15.43% for the mixture containing 15% GGBFS. Initially, the MR of the subgrade soil was calculated. The correlation MR (psi)=2555(CBR)0.64, provided in the third edition of the Mechanistic-Empirical Pavement Design Guide (MEPDG-3, 2024), which includes AASHTO's mechanistic-empirical technical revisions, was employed for this calculation [39]. The calculated MR values were 7,527 psi (51,912,166 Pa) for the unamended soil and 14,709 psi (101,441,717 Pa) for the 15% GGBFS-stabilized mixture. Using Eq. 1 and the data presented in Table 9, the required structural number SN_3 for the subgrade was determined to be 8.40 in (21.34 cm) for the unamended soil and 6.70 in (17.02 cm) for the 15% GGBFS-stabilized soil. The parameters used for the flexible pavement calculations in Table 9 were adopted from KGM (2008). For the calculations, a four-lane (2 × 2) highway with a 20-year design period was considered. The first-year daily traffic consisted of 1,479 trucks, 1,270 trailers, 1,530 minibuses, 1,310 buses, and 4,560 passenger cars, resulting in an equivalent standard axle repetition of 90,000,000. In addition, the criteria selected for the designs were based on AASHTO 1993 [31] and the KGM Flexible Pavement Design Guide [40]. The relevant data were arranged based on values close to the traffic volume of the Kayseri–Nevşehir highway, using the 2024 KGM State Highways Traffic Volume Map data.

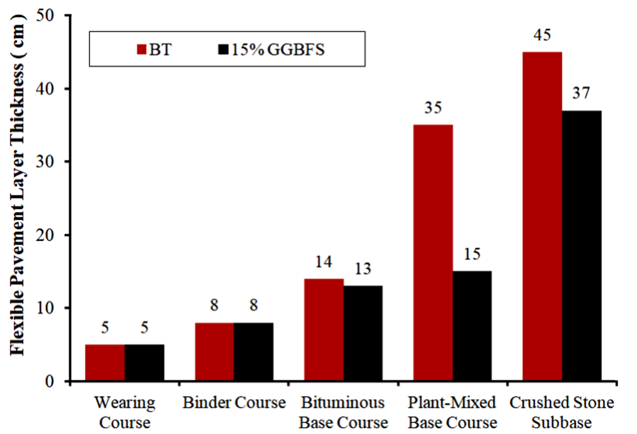

Figure 11. Selected layer thicknesses for untreated soil and 15% GGBFS-stabilized soil.

Table 9. Flexible pavement design parameters.

Parameters	Selected Values
$T_{8.2}$, Number of repetitions of standard single axle load	90,000,000
P_o, Initial serviceability of the pavement	4.2
S_o, Combined standard error of the performance prediction	0.45
Pt, Terminal serviceability of the pavemen	2.5
ΔPSI, Total serviceability loss	1.7
Z_R, Standard normal deviate for reliability	-3.090

3.4.1 Calculation of Layer Thicknesses

Using the SN_3 values obtained for the untreated soil and the soil stabilized with 15% GGBFS, flexible pavement layer thicknesses were calculated based on the MR values derived from the CBR results after 7 days of curing, in accordance with Eq. 1. The selected layer thicknesses are presented in Table 10 and Table 11, respectively. In addition, the layer thicknesses are illustrated in Fig. 11. The structural number (SN) values were determined using Eq. 1. The SN^*

values were calculated based on the layer thicknesses selected in the design. The verification of layer thicknesses was conducted based on CBR values of 50 for the crushed stone subbase and 120 for the plant-mix crushed stone base. Accordingly, the resilient modulus values were calculated as MR = 31,241 psi and MR = 54,710 psi, respectively. Using Eq. 1, the required structural numbers were determined as $SN_1 = 11.88\ cm$ for the plant-mix base and $SN_2 = 9.93\ cm$ for the crushed stone subbase. As a result of the verification, for the untreated soil, the values of $10.34 > 9.93$ for the plant-mix base and $15.59 > 11.89$ for the crushed stone subbase were obtained. For the soil stabilized with 15% GGBFS, the corresponding values were $9.98 > 9.93$ for the plant-mix base and $12.23 > 11.89$for the crushed stone subbase. These results indicate that the flexible pavement layer thicknesses are sufficient. Moreover, stabilization with 15% GGBFS resulted in a 27.10% reduction in the total pavement layer thickness.

Table 10**.** Calculated layer thicknesses and design details for the untreated soil. $SN^* > SN(21.44 > 21.34)$ (The flexible pavement layer thicknesses were appropriately selected).

Layer Name	D_i (cm)	a_i	$SN^* = a_i \times D_i$
Wearing Course	5	0.42	2.10
Binder Course	8	0.40	3.20
Bituminous Base Course	14	0.36	2.04
Plant-Mixed Base Course	35	0.15	5.25
Crushed Stone Subbase	45	0.13	5.85

Table 11**.** Calculated layer thicknesses and design details for the untreated soil. $SN^* > SN(17.04 > 17.02)$ (The flexible pavement layer thicknesses were appropriately selected).

Layer Name	D_i (cm)	a_i	$SN^* = a_i \times D_i$
Wearing Course	5	0.42	2.10
Binder Course	8	0.40	3.20
Bituminous Base Course	13	0.36	4.68
Plant-Mixed Base Course	15	0.15	2.25
Crushed Stone Subbase	37	0.13	4.81

3.5 Economic analysis of flexible pavement design

In order to evaluate the effect of GGBFS-stabilized soil on the construction cost of flexible pavements, an initial construction cost analysis was conducted using the unit price items of the General Directorate of Highways (KGM) [41]. These unit prices were preferred because they adequately meet the project requirements and represent a financial system that is officially accepted by the Republic of Türkiye and compatible with internationally recognized work items. The unit costs per square meter of flexible pavement structures were calculated for untreated soil and soil stabilized with 15% GGBFS. The results are presented in Table 12 and Table 13. In addition, for the stabilization of the subgrade with 15% GGBFS at a thickness of 15 cm, the analysis considered material transportation, soil loosening using a tractor ripper, distribution of the stabilizing material by a bulldozer, spreading and mixing with a grader, watering using a water truck, and compaction using vibratory and pneumatic-tired rollers. Considering that GGBFS is a waste material, its transportation from a maximum distance of 500 km (taking into account the distance between İskenderun Iron Steel Factory and Kayseri and on-site transportation) to the construction site was calculated based on the 2026 cost estimation methodology of the Ministry of Environment, Urbanization, and Climate Change. For international comparison, it is recommended that costs be calculated based on the exchange rate of 1 USD = 43.54 TL according to the data of the Central Bank of the Republic of Türkiye (February 2026). The unit costs of stabilization per square meter are presented in Table 14. Furthermore, a comparative graph of layer costs for untreated soil and soil stabilized with 15% GGBFS is illustrated in Fig. 12. The pavement costs for untreated soil and soil stabilized with 15% GGBFS were determined to be 1,617.93 TL/m^2 and 1,245.07 TL/m^2, respectively. In addition, the cost of the subgrade stabilized with 15% GGBFS was calculated as 37.04 TL/m^2. Considering these costs, a reduction of 23.03% in the initial construction cost was achieved. Based on the calculations, it was estimated that a flexible pavement design constructed on a subgrade improved with 15% GGBFS, with a width of 20 m and a length of 1,000 m, would result in a total cost saving of 7,451,200 TL (approximately 171,134.58 USD).

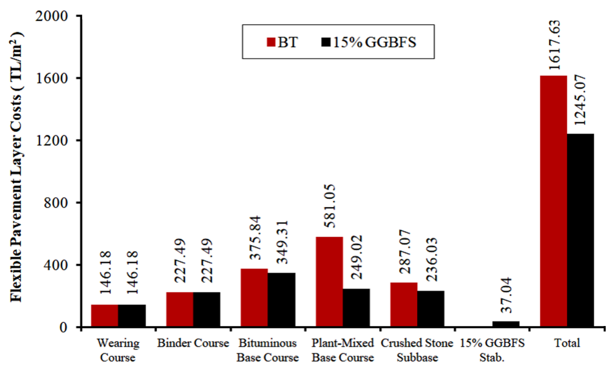

Figure 12**.** Costs of selected layer thicknesses for untreated soil and 15% GGBFS-stabilized soil.

Table 12**.** Pavement layer thickness costs for untreated soil.

Item No.	Course Description	Unit	Unit Price (TL)	Cost (TL/m^2)
KGM/6405	Wearing, 5cm	m^2	146.18	146.18
KGM/6308	Binder, 8cm	m^2	227.49	227.49
KGM/6214	Bituminous Base, 14cm	m^2	375.84	375.84
KGM/6100/3	Plant-Mixed Base, 35cm	ton	691.72	581.05
KGM/6000	Crushed Stone Subbase, 45cm	m^3	637.93	287.07
			Total	**1617.63**

Table 13**.** Pavement layer thickness costs for soil stabilized with 15% GGBFS.

Item No.	Course Description	Unit	Unit Price (TL)	Cost (TL/m^2)
KGM/6405	Wearing, 5cm	m^2	146.18	146.18
KGM/6308	Binder, 8cm	m^2	227.49	227.49
KGM/6214	Bituminous Base, 13cm	m^2	375.84	349.31
KGM/6100/3	Plant-Mixed Base, 15cm	ton	691.72	249.02
KGM/6000	Crushed Stone Subbase, 37m	m^3	637.93	236.03
			Total	**1208.03**

Table 14. Unit stabilization costs for soil stabilized with 15% GGBFS.

Item No.	Description	Unit	Unit Price (TL)	Cost (TL/m^2)
KGM/03.507	Hourly Cost of Tractor Ripper	*h*	3389.77	0.51
KGM/03.511	Hourly Cost of Bulldozer	*h*	3141.42	2.12
KGM/15.140	Mechanical Spreading and Mixing	m^3	22.88	3.43
KGM/15.047	Watering by Water Truck	*ton*	168.98	2.53
KGM/15.052/3	Compaction Using Vibratory Roller	*h*	2722.76	4.08
KGM/15.058/1	Compaction Using Pneumatic-Tired Roller	*h*	2116.99	3.18
Market Price	Supply and Transportation of 15% GGBFS	*kg*	0.85	21.19
			Total	**37.04**

4. Conclusions and recommendations

In this study, the effects of stabilizing bentonite subgrade soil with ground granulated blast furnace slag (GGBFS) on flexible pavement layer thickness and initial construction cost were investigated. The main findings of this study are summarized as follows:

- The results of the Standard Proctor tests indicated that the optimum moisture content increased and the maximum dry density decreased with increasing GGBFS content. This behavior is attributed to the low specific gravity, porous structure, and void-increasing effect of GGBFS, which reduced the compactability of the mixtures and increased their water demand.
- The unconfined compressive strength test results showed that the highest strength values were obtained in samples containing 15% GGBFS after 3 and 7 days of curing. Compared to untreated soil, the strength increased by 2.24 and 2.66 times, respectively, depending on the curing period.
- It was observed that the stiffness of the specimens increased with increasing curing time and GGBFS content, resulting in a decrease in axial strain at failure.
- According to the CBR test results, the CBR values of soils stabilized with 15% GGBFS increased by 2.09 and 2.85 times after 3 and 7 days of curing, respectively, compared to untreated soil. This improvement indicates that GGBFS significantly enhances the bearing capacity of subgrade soils.
- The improvement in mechanical properties and the significant increase in strength values are attributed to the hydraulic and pozzolanic characteristics of GGBFS. It is considered that the reactive components of GGBFS, particularly calcium, silica, and alumina, promote the formation of binder hydration products between bentonite particles. This chemical process is believed to lead to the formation of a stable matrix in highly plastic clay soils, thereby effectively enhancing mechanical strength.
- The pavement design results indicated that a reduction in total pavement layer thickness was achieved for soils stabilized with 15% GGBFS. This reduction is attributed to the positive effect of GGBFS on the bearing capacity of the subgrade.
- The cost analysis revealed that the use of 15% GGBFS-stabilized soil resulted in a cost saving of 23.03% in pavement construction compared to untreated soil. Based on these calculations, it was estimated that stabilizing the subgrade with 15% GGBFS along a divided highway with a width of 20 *m* and a length of 1,000 *m* would lead to a total pavement cost saving of 7,451,200 TL (approximately 171,134.58 USD).
- Overall, the results demonstrate that the stabilization of subgrade soils using waste materials such as GGBFS significantly improves bearing capacity while reducing pavement layer thickness and construction costs. Furthermore, utilizing GGBFS as a stabilization material contributes to waste management and reduces the amount of construction materials required for flexible pavement construction. Consequently, this approach may help decrease CO_2 emissions during the construction phase and support environmental sustainability. With increased adoption of GGBFS in pavement design, further reductions in maintenance and life-cycle costs of highway projects can also be expected.

Authors' contribution

All authors contributed equally to the preparation of this article.

Declaration of competing interest

The authors declare no conflicts of interest.

Funding source

This study didn't receive any specific funds.

Data availability

The data that support the findings of this study are available from the corresponding author upon reasonable request.

REFERENCES

[1] A. Tunç, *Geotechnics and Applications in Highway Engineering*. Nobel Publishing, 2002.

[2] B. Kök, *Highway Engineering and Design*. Nobel Academic Publishing, 2019.

[3] T. Geçkil, T. Sarıcı, and B. Karabaş, "Investigation of the effects of soil improvement with metakaolin on rigid pavement thickness and cost," *Black Sea Journal of Engineering and Science*, vol. 7, no. 5, pp. 11–12, 2024. [Online]. Available: https://doi.org/10.34248/bsengineering.1495259

[4] B. Karabaş, "Effects and sustainability of subgrade soils stabilized with various additives on highway pavements," Ph.D. dissertation, İnönü University, Institute of Natural Sciences, 2025.

[5] T. Sengul, N. Akray, and Y. Vitosoglu, "Investigating the effects of stabilization carried out using fly ash and polypropylene fiber on the properties of highway clay soils," *Construction and Building Materials*, vol. 400, p. 132590, 2023. [Online]. Available: https://doi.org/10.1016/j.conbuildmat.2023.132590

[6] B. Al-Hameidawi, H. Aodah, and H. Shala, "Experimental and numerical evaluation for improvement of underlying layers of road pavement using jute fibre sheets," *Al-Qadisiya Journal for Engineering Sciences*, vol. 9, pp. 461–478, 2016.

[7] M. Al-Zairjawi, "Effect of adding cement and silica fume with cement on compaction properties and shear strength of clayey soil," *Al-Qadisiya Journal for Engineering Sciences*, vol. 2, no. 2, pp. 253–261, 2009.

[8] D. Mohammed, B. Ahmed, and M. Al-Hadidi, "Improving gypseous soil properties by using non-traditional additives," *Al-Qadisiyah Journal for Engineering Sciences*, vol. 12, no. 4, pp. 207–213, 2019. [Online]. Available: https://doi.org/10.30772/qjes.v12i4.637

[9] S. Nugroho, S. Wardani, and A. Muntohar, "Density, load, and fly ash effect on stabilization of high plasticity soil with lime," *Al-Qadisiyah Journal for Engineering Sciences*, vol. 16, no. 2, pp. 102–107, 2023. [Online]. Available: https://doi.org/10.30772/qjes.v16i2.925

[10] M. Rahgozar, M. Saberian, and J. Li, "Soil stabilization with non-conventional eco-friendly agricultural waste materials: An experimental study," *Transportation Geotechnics*, vol. 14, pp. 52–60, 2017. [Online]. Available: https://doi.org/10.1016/j.trgeo.2017.09.004

[11] Zorluer and S. Gucek, "The usability of industrial wastes on soil," *Revista de la Construcción*, vol. 19, no. 1, pp. 80–89, 2020. [Online]. Available: https://doi.org/10.7764/rdlc.19.1.80-89

[12] T. Geçkil, T. Sarıcı, and B. Karabaş, "Effect of black carbon-stabilized subgrade on flexible pavement cost," *European Journal of Science and Technology*, vol. 23, pp. 222–235, 2021. [Online]. Available: https://doi.org/10.31590/ejosat.862682

[13] T. Geckil, T. Sarıcı, and B. Karabas, "Effects of black carbon stabilization on rigid pavement thickness and cost," *ECJSE*, vol. 8, no. 3, pp. 1372–1384, 2021. [Online]. Available: https://doi.org/10.31202/ecjse.894046

[14] S. Perera, M. Saberian, J. Zhu, R. Roychand, and J. Li, "Effect of crushed glass on the mechanical and microstructural behavior of highly expansive clay subgrade," *Case Studies in Construction Materials*, vol. 17, 2022. [Online]. Available: https://doi.org/10.1016/j.cscm.2022.e01244

[15] R. Domphoeun and A. Eisazadeh, "Flexural and shear strength properties of laterite soil stabilized with rice husk ash, coir fiber, and lime," *Transportation Infrastructure Geotechnology*, 2024. [Online]. Available: https://doi.org/10.1007/s40515-023-00364-5

[16] O. Sivrikaya, S. Yavascan, and E. Cecen, "Effects of ground granulated blast-furnace slag on the index and compaction parameters of clayey soils," *Acta Geotechnica Slovenica*, vol. 11, no. 1, pp. 19–27, 2014.

[17] S. Abdila *et al.*, "Potential of soil stabilization using ground granulated blast furnace slag (ggbfs) and fly ash via geopolymerization method: A review," *Materials*, vol. 15, no. 1, p. 375, 2022.

[18] A. Soğancı, Y. Yenginar, and A. Orman, "Geotechnical properties of clayey soils stabilized with marble dust and granulated blast furnace slag," *KSCE Journal of Civil Engineering*, vol. 27, no. 11, pp. 4622–4634, 2023. [Online]. Available: https://doi.org/10.3390/ma15010375

[19] L. d. S. Tomaz, P. d. S. Machado, A. d. D. Fraga, G. Souza, and H. Diniz, "Analysis of compaction of stabilized soils using blast furnace slag," *Journal of Engineering and Exact Sciences*, vol. 11, no. 1, 2025. [Online]. Available: https://doi.org/10.18540/jcec

[20] J. Hu *et al.*, "Machine learning-based optimization of geopolymer-stabilized soil formulation using blast furnace slag and fly ash," *Materials Today Communications*, p. 113500, 2025. [Online]. Available: https://doi.org/10.1016/j.mtcomm.2025.113500

[21] A. Uzer *et al.*, "Sustainable stabilization of clay soils using fly ash and blast furnace slag-based geopolymers: Comprehensive experimental evaluation and artificial neural network modelling," *Structural Engineering and Mechanics*, vol. 96, no. 1, pp. 13–33, 2025. [Online]. Available: https://doi.org/10.12989/sem.2025.96.1.013

[22] ASTM International-D4318, "Astm d4318: Standard test methods for liquid limit, plastic limit, and plasticity index of soils," ASTM International, West Conshohocken, PA, Tech. Rep., 2017.

[23] ASTM International-D698, "Astm d698: Standard test methods for laboratory compaction characteristics of soil using standard effort," ASTM International, West Conshohocken, PA, Tech. Rep., 2014.

[24] ASTM International-D854, "ASTM D854: Standard test method for specific gravity of soils," ASTM International, West Conshohocken, PA, Tech. Rep., 2006.

[25] ASTM International-D6913, "ASTM D6913: Standard test methods for particle-size distribution (gradation) of soils using sieve analysis," ASTM International, West Conshohocken, PA, Tech. Rep., 2017.

[26] Yılmaz, M. Yıldıran, and Keskin, *Soil Mechanics Laboratory Experiments and Solved Problems*. Seçkin Publishing, 2017.

[27] ASTM International-D2166-06, "ASTM D2166-06: Standard test method for unconfined compressive strength of cohesive soil," ASTM International, West Conshohocken, PA, Tech. Rep., 2006.

[28] M. Orhan, *Soil Mechanics Laboratory Experiments*. Gazi Publishing, 2013.

[29] ASTM International-D1883-21, "ASTM D1883-21: Standard test method for california bearing ratio (cbr) of laboratory-compacted soils," ASTM International, West Conshohocken, PA, Tech. Rep., 2021.

[30] T. Geçkil, T. Sarıcı, and B. Karabaş, "Investigation of the effect of pumice-stone-stabilized sandy soil on flexible pavement design," *International Journal of Pure and Applied Sciences*, vol. 11, no. 1, pp. 176–192, 2025. [Online]. Available: https://doi.org/10.29132/ijpas.1629437

[31] American Association of State Highway and Transportation Officials (AASHTO), "Guide for design of pavement structures (interim)," AASHTO, Washington, DC, Tech. Rep., 1993.

[32] T. Geçkil, T. Sarıcı, and B. Karabaş, "Investigation of layer thickness and cost of flexible pavement designed on glass-powder-improved soil," *Journal of Innovative Engineering and Natural Science*, vol. 5, no. 1, pp. 81–99, 2025. [Online]. Available: https://doi.org/10.61112/jiens.1509488

[33] M. Tanyıldızı, "Effects of blast furnace slag stabilization on flexible pavement thickness and cost," *Fırat University Journal of Engineering Sciences*, vol. 32, no. 2, pp. 509–520, 2020. [Online]. Available: https://doi.org/10.35234/fumbd.738512

[34] E. Hamed and A. Demiröz, "Optimization of geotechnical characteristics of clayey soils using fly ash and granulated blast furnace slag-based geopolymer," *Construction and Building Materials*, vol. 441, p. 137488, 2024. [Online]. Available: https://doi.org/10.1016/j.conbuildmat.2024.137488

[35] M. Shakil, S. Nazar, H. Ameen, A. Shahzad, and F. Ahmad, "A comparative study of ground granulated blast furnace slag and bagasse ash incorporation on enhancing mechanical properties of expansive soil," *Results in Engineering*, vol. 25, p. 103569, 2025. [Online]. Available: https://doi.org/10.1016/j.rineng.2024.103569

[36] T. Sarıcı, T. Geçkil, B. Ok, and H. Aksoy, "An investigation of the usability of alkali-activated blast furnace slag-additive construction demolition waste as filling material," *Materials*, vol. 18, no. 2, p. 398, 2025. [Online]. Available: https://doi.org/10.3390/ma18020398

[37] W. Sas, J. Dzieciol, A. Radzevičius, M. Radziemska, M. Dapkienė, R. Šadzevičius, and A. Głuchowski, "Geotechnical and environmental assessment of blast furnace slag for engineering applications," *Materials*, vol. 14, no. 20, p. 6029, 2021. [Online]. Available: https://doi.org/10.3390/ma14206029

[38] B. Uzuner, *Introduction to Foundation Engineering*. Derya Publishing, 2016.

[39] American Association of State Highway and Transportation Officials (AASHTO), "Mechanistic–empirical pavement design guide (3rd ed., mepdg-3)," AASHTO, Washington, DC, Tech. Rep., 2024.

[40] General Directorate of Highways (KGM), "Highways flexible pavement project design guide," General Directorate of Highways (KGM), Technical Research Department, Pavement Branch, Ankara, Turkey, Tech. Rep., 2008.

[41] KGM, "General directorate of highways-unit prices," Ankara, 2026. [Online]. Available: http://www.kgm.gov.tr

How to cite this article:
Bahadır Karabaş, Ali Ulvi Uzer, (2026). 'Effect of ground granulated blast furnace slag–stabilized bentonite soils on flexible pavement design and cost analysis', Al-Qadisiyah Journal for Engineering Sciences, 19 (2), pp. 195- 202. https://doi.org/10.30772/qjes.2026.169263.1896